ISSN 1063-7834, Physics of the Solid State, 2021. © Pleiades Publishing, Ltd., 2021.
Russian Text © The Author(s), 2021, published in Fizika Tverdogo Tela, 2021, Vol. 63, No. 9, pp. 1223–1227.

SUPERCONDUCTIVITY

Development of Josephson Traveling-Wave Parametric Amplifier Based on Aluminum SIS Junctions

M. Tarasov[a], *, A. Gunbina[b], S. Lemzyakov[c], D. Nagirnaya[a], M. Fominskii[a], A. Chekushkin[a], V. Koshelets[a], E. Goldobin[d], and A. Kalaboukhov[e]

[a] *Kotel'nikov Institute of Radio Engineering and Electronics, Russian Academy of Sciences, Moscow, Russia*
[b] *Institute of Applied Physics, Russian Academy of Sciences, Nizhny Novgorod, Russia*
[c] *Kapitsa Institute of Physical Problems, Russian Academy of Sciences, Moscow, Russia*
[d] *Eberhard Karl University of Tübingen, Tübingen, DE72074 Germany*
[e] *Chalmers University of Technology, Gothenburg, SE-412 96 Sweden*
**e-mail: tarasov@hitech.cplire.ru*

Received April 9, 2021; revised April 9, 2021; accepted April 19, 2021

Abstract—Prototypes of the design of Josephson traveling-wave parametric amplifier based on aluminum superconductor–insulator–superconductor junctions in the form of direct-current SQUIDs included in central conductor of coplanar line are developed, fabricated, and investigated. Three manufacturing methods for the fabrication of such devices are tested: two of them using shadow evaporation and one using magnetron sputtering and direct electron-beam lithography. Current–voltage characteristics of the junctions are measured at 0.3 K. A cryogenic setup for the measurement of spectral characteristics of such amplifier containing cold semiconductor amplifier with circulator and cooled attenuators of the channels of input signal and pump is developed. The absorption spectrum of coplanar directional coupler with a quarter-wave resonator dedicated for measurements of short chains from one to 27 SQUIDs is measured.

Keywords: superconductor tunnel junctions, SQUIDs, Josephson traveling-wave parametric amplifiers, SIS junctions, magnetron sputtering

DOI: 10.1134/S1063783421090419

INTRODUCTION

Semiconductor microwave amplifiers could not provide noise characteristics necessary for the development of qubit readout systems, axion detectors, and the frequency-division multiplexing systems of the matrices of cryogenic bolometers. Application of Josephson SIS junctions could implement nonlinear inductance without losses and provides the characteristics, which could not be achieved for dissipative nonlinear elements. Development of broadband Josephson microwave traveling-wave amplifier could circumvent band and dynamic-range constraints, which exist for conventional lumped-element parametric amplifier, and decrease noises below the quantum limit. Recent theoretical works [1] have shown the potential of circumvention of these restrictions and give the amplification up to 20 dB at the bandwidth higher than 5 GHz. A fundamental possibility of bandwidth enhancement of Josephson parametric amplifier up to 4 GHz at the gain of up to 17 dB was experimentally demonstrated in [2]. A more difficult problem is the development of the prototype of such amplifier, which operates at milli-Kelvin temperatures and possesses the noise temperature close to the quantum limit of less than 0.5 K at the frequency of around 8 GHz, which is the aim of this work.

CHOICE OF MATERIAL AND TECHNOLOGY FOR VARIOUS APPLICATIONS

When Josephson traveling-wave parametric amplifier (JTWPA) is used as the intermediate-frequency amplifier (IFA) of SIS mixer or in the bolometer readout system at the temperature of liquid helium, niobium or its nitrides are a natural choice of the amplifier material. In this case, JTWPA mounted at the same temperature step with the first cascade, which allows one to make the intermediate-frequency sections shorter and remarkably reduce the consumed power as compared to semiconductor amplifiers, which dissipate a significant power. In the case of helium temperatures, there is a well-developed single-pumpdown technology for niobium three-layer structure Nb–AlO_x–Nb, which involves magnetron sputtering, plasma-chemical etching of niobium, and plasma or ion beam etching of aluminum. However, employment of niobium amplifiers along with high power supply at milli-Kelvin temperatures is associ-

ated with the problems of high thermal load on the low-temperature step or additional losses in long intermediate-frequency sections between the low-temperature step with the first cascade and the step with the temperature of 3 K, on which IFA is located. Josephson SIS junctions based on aluminum with the critical temperature of 1.2 K could be favorable for the application as the readout channels of milli-Kelvin bolometers, axion detectors, and qubits, which require the working temperatures of 0.1 K and lower.

When there is identical area of junctions and identical oxidation conditions, asymptotic resistance of niobium and aluminum junctions is equivalent, because aluminum oxide or nitride are used as tunneling barriers in both cases. Whereas critical currents differ from each other as the ratio of critical temperatures, that is, nearly by the factor of eight. In the case of a typical SIS junction with the area of 4.5 μm^2 and asymptotic resistance of 230 Ω, critical current corresponds to 12 μA for niobium and 1.5 μA for aluminum. The main parameter at the design of JTWPA is a nonlinear inductance of Josephson junction and it could be larger for aluminum by the factor of eight at the same size of junctions. The dissipated power, which is proportional to the square current, that is, differs by the factor of 64, is an important parameter for cryogenic amplifier. Eight aluminum junctions are necessary for niobium to achieve necessary nonlinearity, while one aluminum junction is sufficient in other cases; as a result, heat release differs by the factor of 512.

In the case of aluminum SIS junctions, the pump power would be less by the same factor as compared to niobium ones. The number of junctions in the chain is determined by the amplification coefficient per one cell g_0, which is determined by the following equation at optimal inductance parameter $\beta_L \approx 1$ and the pump amplitude $I_p/I_c = 0.5$: $g_0 = (1/16)f_p/f_0$, where $f_0 = Z_0 2I_c/\Phi_0$, $Z_0 = 50$ Ω, and $\Phi_0 = 2 \times 10^{-15}$ Wb. As a result, we have $g_0 \propto 1/I_c$; i.e., amplification per one cell is eight times as large for aluminum SIS under other conditions being equal and eight times lower number of cells is necessary as compared to niobium SIS.

Smearing of CVCs by thermal noises for Josephson junction is determined by the band width, in which noises affect the Josephson junction, and corresponds to $0.7eV_\Delta/h$ (where e is the charge of electron, V_Δ is the voltage corresponding to the energy gap, and h is Planck constant), that is, ca. 500 GHz for niobium and 50 GHz for aluminum, that is, one order of magnitude lower. The working temperature of niobium junction is 4 K and that of aluminum is 0.3 K. As a result, smearing of CVCs of niobium junction at helium temperature is ca. 0.4 μA, while that of aluminum is ca. 5 nA at 0.3 K, that is, two orders of magnitude lower.

An important advantage of aluminum superconducting structures is the absence of frozen-in quanta of magnetic flux for the films that are thicker than a double London penetration depth. This thickness is larger than 100 nm for aluminum and our samples are 300 nm thick. In the case of niobium films, which is the type-II superconductor, the presence of Abrikosov vortices is inevitable, which results in additional noises arising at spontaneous motion of vortices.

Thus, the use of aluminum structures is favorable for the achievement of limiting characteristics of JTWPAs, whereas niobium constructions allow quick development of circuit engineering and test these amplifiers at the temperature of liquid helium without the use of complex sorption cryostats and dilution refrigerators. Niobium amplifiers can be used as a second stage cascade of amplification at the temperature level of 3 K, which could provide both temperature decoupling and additional amplification. In the case of a three-step amplification at 0.3, 3, and 70 K using aluminum JTWPA, niobium JTWPA, and semiconductor amplifier, one can restrict to power gain of ca. 10 dB per each cascade and avoid self-excitation and thermal overheating of the cold step.

TOPOLOGY, TECHNOLOGY, MEASUREMENTS

Aluminum SIS junctions are traditionally fabricated using shadow evaporation with the suspended bridge of resist using Dolan method [3] or according to the bridge-free technology by evaporating into narrow orthogonal grooves in a thick resist [4, 5]. Electron-beam evaporation is carried out at the slope of 45° at two orthogonal positions of plate. After first evaporation, the aluminum layer is oxidized for the formation of tunneling barrier. The grounding capacity of 0.12 pF for the wave impedance of 50 Ω gives the cross-section frequency of 28 GHz; in this case, the plasma frequency corresponds to 12 GHz. In the loop of RF SQUID, there is a SIS junction as a Josephson junction with the area of 10 μm^2 with the critical current of 1 μA and the kinetic inductance of 300 pH at zero bias. As an additional kinetic inductance, four SIS junctions with the critical current of 5 μA or 16 SIS junctions with the critical current of 20 μA are used in order to specify the value of constant magnetic flux using the bias current of 10 μA, which corresponds to one-half of the quantum of magnetic flux. Figure 1a shows the optical image of one SQUID element of amplifier, in which the inductance of SQUID loop consists both of geometrical inductance and kinetic inductance of four Josephson SIS junctions (measured CVC of individual SIS junction is given in Fig. 1b).

The described technology of shadow evaporation at industrial scale is not employed due to high labor consumption and low reproducibility. A standard technology of superconductor integral circuits based on niobium and it's nitrides employs magnetron sputtering. However, until recently, analogous process was

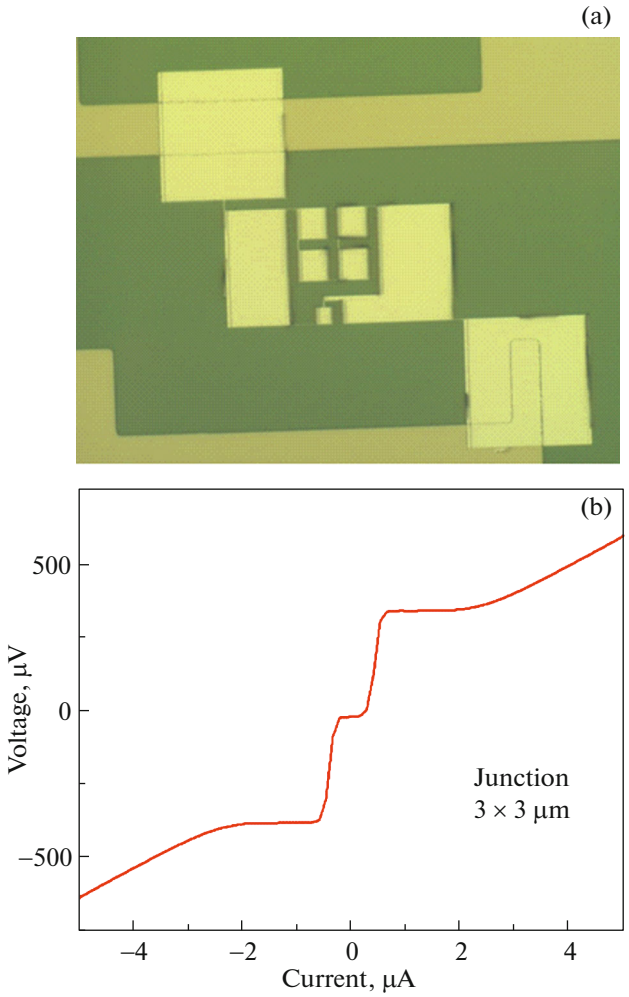

Fig. 1. JTWPA fabricated by shadow evaporation with additional kinetic inductances based on SIS junctions: (a) optical image of element and (b) measured CVC of the junction with the size of 3 × 3 μm at the temperature of 0.28 K.

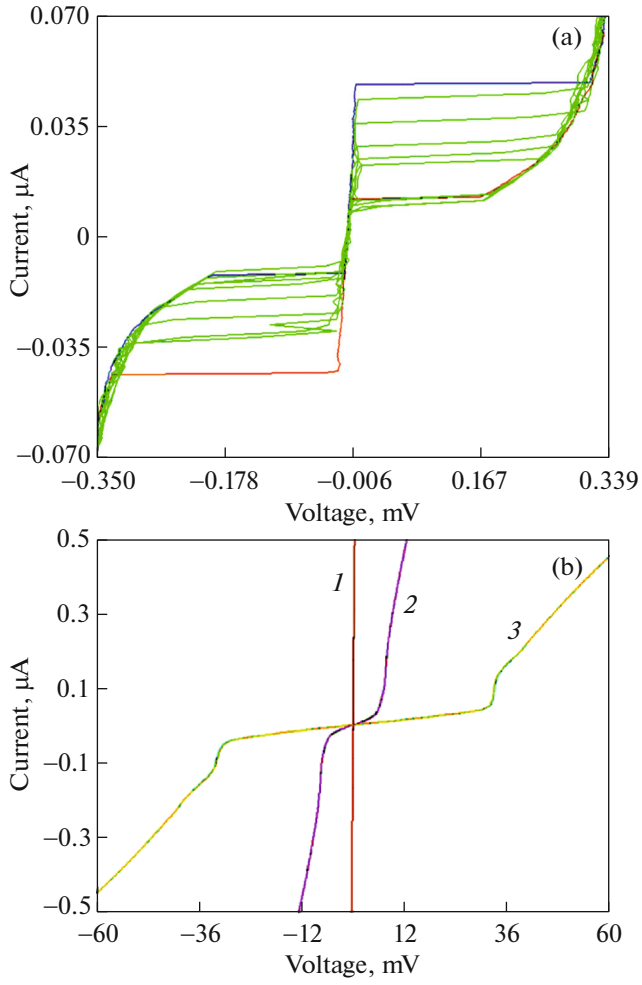

Fig. 2. (a) Current–voltage characteristics of one SQUID at different values of external magnetic flux: from zero (curve with the maximum critical current) to the one corresponding to one-half of the quantum of magnetic flux (the curve with the minimum critical current); (b) current–voltage characteristics of the different chains: (*1*) 10, (*2*) 20, and (*3*) 100 SQUIDs. The samples were fabricated using magnetron sputtering and direct electron-beam lithography.

not implemented for aluminum SIS structures. We have developed the following fabrication map: the topology of lower electrode is formed by the first lithography and the first aluminum electrode with the thickness of 300 nm is subsequently exposed and sputtered. Second lithography opens windows over the first aluminum layer and ion beam or plasma etching of natural aluminum oxide and a small layer of pure aluminum is performed; after that, surface aluminum is oxidized for the formation of a tunneling barrier; the upper aluminum layer with the thickness of 350 nm is further sputtered into the same windows. Current–voltage characteristics of the element of the SQUID chain integrated in coplanar line are given in Fig. 2. In order to verify the process compatibility and study different operating conditions of SQUIDs, several variants of the topology of the samples were designed, which include coplanar lines with the SQUID chains and parallel coplanar lines for the supply of the pump power and constant magnetic field. In addition to the transmission line, the variants with quarter-wave coplanar resonator with different length of chains were designed (including 1, 10, 100, and 350 SQUIDs). The junction sizes varied from 1 × 1 to 2 × 2 μm (critical currents are 0.3–1.2 μA, Josephson kinetic inductance is 600–200 pH), and geometrical loop is from 50 to 260 μm^2 (ca. 10 and 20 pH). Such technology, in contrast to shadow evaporation allows one to sputter sufficiently thick electrodes of 300 nm. The SQUIDs with the junctions of 2 × 2 μm possessed the normal resistance of 360 Ω; with the junctions of 1 × 1 μm,

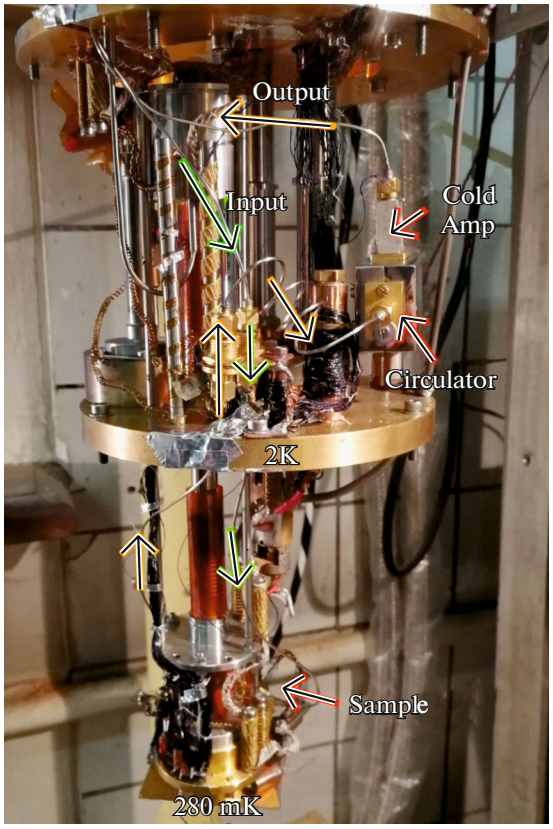

Fig. 3. Photograph of the cryostat with input and output coaxial transmission lines, cold semiconductor amplifier with the circulator at the step of 3 K, and the sample at the step of 280 mK.

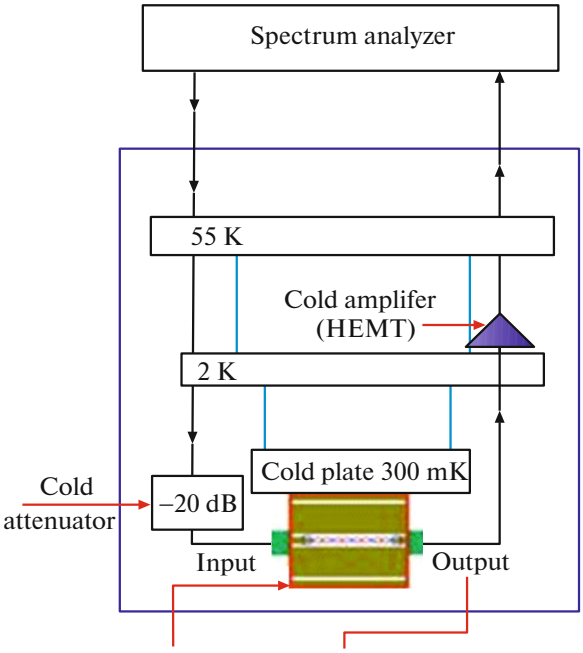

Fig. 4. Block diagram of the measurement setup for the study of JTWPA per one run. The sample and cold attenuator are located at the step of 300 mK and cold semiconductor amplifier with the circulator at the step of 2 K.

600 Ω; the chains made from 10 SQUIDs, 6 kΩ; from 20 SQUIDs, 12 kΩ; and from 100 SQUIDs, 58 kΩ, which indicates a sufficient reproducibility of the structures fabricated according to this technology.

For measuring of the fabricated samples, we employed the modified measuring setup that was developed for the investigation of the bolometers with microwave readout [6, 7], see photo in Fig. 3 and block diagram in Fig. 4. A HELIOX-AC-V Oxford Instruments cryostat was equipped with coaxial lines with filters, attenuators, and cold amplifier with the circulator at input. To perform measurements at direct current, the resistors of 500 kΩ cooled to the temperature of the sample of 0.3 K connected by twisted pairs to the symmetrical source for the bias specification and measurement of CVCs. Measurements and tuning of the section elements were performed using an ARINST VNA-PR1 dual-port vector network analyzer and an ARINST SSA-TG R2 spectrum analyzer of KROKS Company (Voronezh). Unloaded Q-factor corresponded to ca. 200. The presence of the SQUID chain in the central line results in the variations of Q-factor and frequency depending on constant magnetic flux and pump power.

Further optimization of structure suggests the study of a bi-SQUID as a basic element [8], which contains a standard dc-SQUID and additional Josephson junction, which partially bypasses the geometric inductance of the loop by the kinetic inductance that is two to four times as large as geometrical. According to the theory from [8], such type of SQUID can improve linearity of signal characteristics and expand the dynamic range of entire amplifier.

FUNDING

The work was supported by the State Assignment of the Institute of Radio Engineering and Electronics of the Russian Academy of Sciences (no. 030-2019-0003) and the State Assignment of the Institute of Applied Physics of the Russian Academy of Sciences. Fabrication, development, and investigation of the specimens were supported by the Russian Science Foundation grant no. 21-42-04421 based on a unique scientific setup (UNU no. 352529). Development of individual elements of the technology of THz detectors was performed by A. Gunbina in the Institute of Applied Physics of the Russian Academy of Sciences within the Russian Science Foundation project no. 19-19-00499.

CONFLICT OF INTEREST

The authors declare that they have no conflicts of interest.

REFERENCES

1. A. B. Zorin, Phys. Rev. Appl. **6**, 034006 (2016).
2. A. Miano and O. Mukhanov, IEEE Trans. Appl. Supercond. **29**, 1501706 (2019).
3. G. Dolan, Appl. Phys. Lett. **31**, 337 (1977).
4. M. Brink, US Patent No. 0358538 A1 (2018).
5. M. Tarasov, A. Gunbina, D. Nagirnaya, and M. Fominskii, RF Patent No. 2019123125 A (2019).
6. M. A. Tarasov, S. Makhashabde, A. A. Gunbina, R. A. Yusupov, A. M. Chekushkin, S. A. Lemzyakov, D. V. Nagirnaya, M. A. Mansfel'd, V. F. Vdovin, V. S. Edel'man, A. S. Kalabukhov, and D. Vinkler, Phys. Solid State **62**, 1580 (2020).
7. A. A. Gunbina, S. Mahashabde, M. A. Tarasov, G. V. Yakopov, R. A. Yusupov, A. M. Chekushkin, D. V. Nagirnaya, S. A. Lemzyakov, V. F. Vdovin, A. S. Kalaboukhov, and D. Winkler, in *Proceedings of the ASC* (2020), Paper Wk2EPo1E-03.
8. V. K. Kornev, I. I. Soloviev, N. V. Klenov, and O. A. Mukhanov, Supercond. Sci. Technol. **22**, 114011 (2009).

Translated by A. Muravev